ALEXANDER VAKHRUSHEV[1], MENGHUAI WU[1], ANDREAS LUDWIG[2], GERALD NITZL[3], YONG TANG[3], GERNOT HACKL[3]

EXPERIMENTAL VERIFICATION OF A 3-PHASE CONTINUOUS CASTING SIMULATION USING A WATER MODEL

Abstract

In the continuous casting (CC) mold, a stable meniscus is crucial so the covering slag layer effectively protects molten steel from oxidation. In practice it is difficult to control due to the special flow pattern in the mold region. Therefore, a modeling approach was investigated to predict and optimize the casting process by stabilizing the meniscus. The volume-of-fluid (VOF) approach was utilized to model the mold flow including the free surface behavior in a 3-phase liquid steel/slag/air system on the basis of the OpenFOAM® finite volume method (FVM) open-source CFD package. Before applying this approach to industry, laboratory experiments with a water model, comprising a 1/3 scaled-down conventional mold, were performed to evaluate the numerical model. An oil layer was used to mimic the slag layer covering the meniscus. The evolution of the meniscus and distribution of the oil layer in response to the mold flow were experimentally recorded. In the numerical model, three phases were considered: water, oil and air. The preliminary simulation results were compared to the water modeling data. Some sensitive parameters for this model such as surface tension (interface free energy) and contact angle were also investigated.

Keywords

Free surface, numerical simulation, VOF, slag entrapment, surface tension, continuous casting

1. Introduction

An accurate representation of the coupled effects between turbulent fluid flow and moving fluid-fluid interfaces is necessary for a realistic prediction/control of the continuous casting process. The evolution of the free interface, slag entrapment etc., makes this a very challenging task. After more than 30 years of numerical model and algorithm development, this is still not a concluded topic in CFD. A review of the wide range of computational methods (unstructured, structured and block-structured) is provided by Cross et al. [1] and reintroduces the challenges of generating rapid solutions with high-performance parallel cluster technology, as well as the computational speed issues when using various methods and different commercial CFD software. In the current studies the volume-of-fluid (VOF) method was employed based on its implementation in the OpenFOAM® open-source CFD software package [2].

Free-surface methodologies can be classified into surface tracking, moving mesh and volume tracking methods [3]:

[1] Christian-Doppler Laboratory for Advanced Process Simulation of Solidification and Melting, University of Leoben, Austria
[2] Chair of Simulation and Modeling of Metallurgy Processes, University of Leoben, Austria
[3] RHI AG, Austria

- surface tracking methods define a sharp interface. The interface is marked and its motion is tracked;
- moving mesh methods couple the interface with a set of nodal points from the computational mesh. In this way, a sharp interface is maintained; the mesh is moved to fit the interface;
- volume tracking methods mark different phases with massless particles or an indicator function, which can be a volume fraction [4], a level set [5] or a phase field [6].

Moving mesh and surface tracking methods maintain the exact position of the interface, which simplifies analysis near the interface. In contrast, the mesh or marker particles have to be relocated and quite often re-meshed when the interface undergoes large deformations, which leads to additional complexity.

Volume tracking methods utilize an indicator function (volume fraction, level set or phase field) to represent the interface. The complexity starts when the convection scheme has to guarantee that the volume fraction stays bound, i.e., remains within its physical bounds between 0 and 1. This problem has been addressed by a number of authors and led to development of the VOF method, which utilizes convection schemes to reconstruct the interface from the volume fraction distribution before advecting it [4].

The surface tension (interface free energy) term in the Navier-Stokes equation creates additional difficulties because it is a singular term. Here, the continuum surface force (CSF) formulation by Brackbill et al., [7] is used to calculate the surface tension force from the distribution of the indicator function.

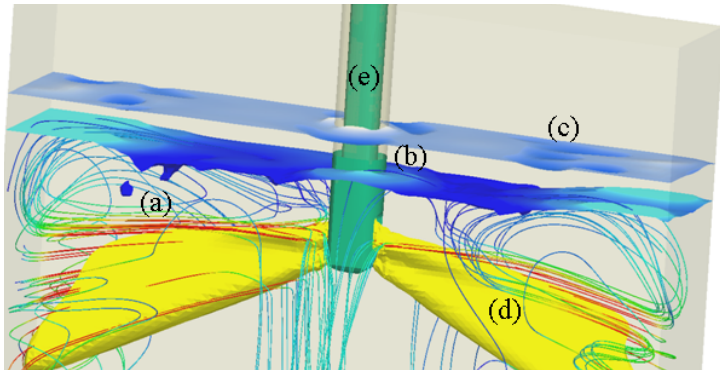

Fig. 1. Examples of flow-related phenomena during continuous casting that can be tracked by means of the VOF multiphase simulation: (a) mechanisms of slag entrapment; (b) SEN refractory erosion kinetics; (c) free surface oscillation/waves; (d) patterns of turbulent jet flow; (e) sensitivity of all the above phenomena to the SEN design.

A comprehensive review and analyzes that focus on the VOF methods to track interfaces in multiphase flows can be found in the work of Gopala et al., [8]. Recently a number of approaches and enhanced numerical schemes were developed by other authors to overcome the limitations of the VOF method by increasing the accuracy of the interface reconstruction using high-order interpolation [9] and to provide a sharper interface with the high density ratios in the order of 1000 to 1 [10], or to introduce interface compressing schemes [11].

The numerical simulation helps to understand many advanced aspects of the multiphase flow phenomenon during the continuous casting process (Fig. 1). Important criteria such as slag entrapment due to the critical casting speed, swirl formation, free surface waves, the

kinetics of SEN refractory erosion, turbulent jet stability and melt mixing mechanisms can be studied and analyzed based on the numerical simulation results.

The objective of this work was to evaluate the capabilities and accuracy of the VOF method when applied to continuous casting (CC) and compare the results with data obtained using water modeling. The mathematical formulation of the 3-phase VOF method, experimental setup of the water model and numerical simulations are presented and compared; challenges and further requirements are also discussed.

2. Numerical model

Implementation of the VOF model was based on work described in the PhD thesis of Ubbink [12] and the Ubbink and Issa publication [13]. Different fluids were modeled as a single continuum obeying the same set of governing equations. Different fluid phases were identified locally by their volume fractions. In this paper a 3-phase (melt or water, slag and air) system was considered. The volume fractions of all phases must sum up to one.

$$\alpha_{\text{melt}} + \alpha_{\text{slag}} + \alpha_{\text{air}} = 1. \tag{1}$$

The mixture properties such as density and dynamic viscosity were calculated as a weighted average according to the volume fractions of the phases:

$$\rho_{\text{mixture}} = \alpha_{\text{melt}} \cdot \rho_{\text{melt}} + \alpha_{\text{slag}} \cdot \rho_{\text{slag}} + \alpha_{\text{air}} \cdot \rho_{\text{air}} \tag{2}$$

$$\mu_{\text{mixture}} = \alpha_{\text{melt}} \cdot \rho_{\text{melt}} \cdot \eta_{\text{melt}} + \alpha_{\text{slag}} \cdot \rho_{\text{slag}} \cdot \eta_{\text{slag}} + \alpha_{\text{air}} \cdot \rho_{\text{air}} \cdot \eta_{\text{air}} \tag{3}$$

Kinematic viscosity was obtained from the mixture's dynamic viscosity and density:

$$\eta_{\text{mixture}} = \mu_{\text{mixture}} / \rho_{\text{mixture}} \tag{4}$$

Hereafter all properties/quantities without subscripts refer to the mixture and those with subscripts correspond to a particular phase. The governing equations of the unsteady, turbulent and incompressible flow for the mixture were as follows:

$$\nabla \cdot \vec{u} = 0 \tag{5}$$

$$\frac{\partial \rho \vec{u}}{\partial t} + \nabla \cdot (\rho \vec{u} \otimes \vec{u}) = -\nabla p + \nabla \cdot (2\mu_{\text{eff}} \mathbf{D}) + \rho \vec{g} + \vec{S}_{\text{surf}} \tag{6}$$

Where $\vec{u}$ is the velocity, p is the pressure and $\vec{g}$ is the gravitational acceleration. The buoyancy force was taken into account using the Boussinesq approximation. The rate of strain tensor was defined by:

$$\mathbf{D} = \frac{1}{2}(\nabla \vec{u} + (\nabla \vec{u})^{\text{T}}) \tag{7}$$

The continuum surface force (CSF) is given according to Brackbill et al. [7] by including the surface tension (interface free energy) as an additional source term, $\vec{S}_{\text{surf}}$, on the right-hand side of the momentum equation (6).

$$\vec{S}_{\text{surf}} = \sigma\kappa\mathbf{n} \tag{8}$$

Where **n** is the interface normal vector that can be estimated from:

$$\mathbf{n} = \nabla\alpha \tag{9}$$

The fraction gradient function $\nabla\alpha$ is continuous and non-zero at the transitional area of the interface only.

The curvature of the interface κ was expressed in terms of the divergence of the unit normal vector as follows:

$$\kappa = -\nabla \cdot \left(\frac{\nabla\alpha}{|\nabla\alpha|}\right). \tag{10}$$

It should be noted that formulas (8)–(10) are valid for the 2-phase system. The numerical implementation in the OpenFOAM® source code includes an incompressible multi-phase mixture with a built-in solution for the arbitrary phases with interface compression to capture the interface [2]. Hence the surface tension force for the interface between each phase pair was evaluated as follows:

$$\vec{S}_{\text{surf}} = \sum_{i,j} \sigma_{ij}\kappa_{ij}\left(\alpha_j\nabla\alpha_i - \alpha_i\nabla\alpha_j\right) \tag{11}$$

for all phase pairs (*i, j*), where the corresponding curvature κ_{ij} was calculated as:

$$\kappa_{ij} = -\nabla \cdot \frac{\left(\alpha_j\nabla\alpha_i - \alpha_i\nabla\alpha_j\right)}{\left|\alpha_j\nabla\alpha_i - \alpha_i\nabla\alpha_j\right|} \tag{12}$$

The formulas (11) and (12) use a pair-averaged gradient of the phase fraction, in comparison to the 2-phase formulas for the interface normal vector (9) and curvature (10):

$$\nabla\alpha|_{ij} = \alpha_j\nabla\alpha_i - \alpha_i\nabla\alpha_j \tag{13}$$

The scalar transport equation of the volume fraction α_i for each phase was:

$$\frac{\partial\alpha_i}{\partial t} + \nabla \cdot (\vec{u}\alpha_i) = 0 \tag{14}$$

A realizable $k-\epsilon$ model was employed for the turbulence, providing improved performance for flow calculations involving boundary layers under strong pressure gradients and strong streamline curvature. The governing equations for the turbulence were:

$$\frac{\partial\rho k}{\partial t} + \nabla \cdot (\rho\vec{u}k) = \nabla \cdot \left(\left(\mu + \frac{\mu_{\text{t}}}{Pr_{\text{t,k}}}\nabla k\right)\right) + G - \rho\epsilon \tag{15}$$

$$\frac{\partial\rho\epsilon}{\partial t} + \nabla \cdot (\rho\vec{u}\epsilon) = \nabla \cdot \left(\left(\mu + \frac{\mu_{\text{t}}}{Pr_{\text{t},\epsilon}}\nabla\epsilon\right)\right) + \rho C_{1\epsilon}\epsilon - C_{2\epsilon}\rho\frac{\epsilon^2}{\sqrt{Sk}} \tag{16}$$

where $S = \sqrt{2D_{ij}D_{ij}}$; the turbulence Prandtl number for k is given as $Pr_{\mathrm{t,k}} = 1$ and for ϵ is given as $Pr_{\mathrm{t},\epsilon} = 1.2$. In equation (15), G is the shear production of turbulence kinetic energy. The influence of turbulence on the momentum transport was considered by the effective viscosity, $\mu_{\mathrm{eff}} = \mu + \mu_{\mathrm{t}}$, where $\mu_{\mathrm{t}} = \rho C_{\mu}\, k^2/\epsilon$; C_{μ} is a function of the velocity gradient and ensures positive normal stresses.

The governing equations of the 3-phase VOF model, including turbulence as described above, were implemented in an OpenFOAM® CFD software package [2] and could be run both in serial mode or in parallel mode using high performance cluster. Some functionalities of the standard solver were extended by the current authors:

- adaptive mesh refinement on the unstructured grids to improve resolution of the interface to track the slag entrapment by the flow;
- dumping the momentum transfer from the slag and melt into the air region.

3. Experimental setup

The laboratory water modeling experiment was performed at the RHI Technology Center (Leoben, Austria). The setup represented a 1/3 scaled-down water model of a conventional CC mold (Fig. 2). The mold was manufactured from transparent material (plexiglass); therefore, it was possible to record evolution of the flow and the free surface during the experiment.

Water was used to mimic the melt due to the fact that the kinematic viscosity of liquid steel and water are similar. The properties of actual materials in CC and their analogs used in the laboratory experiment are listed in Table 1. The properties of real slag are not specified in the table because they are highly temperature, composition and state dependent. For comparison with the water modeling experiment, an isothermal simulation was performed. Therefore all properties corresponded to those at room temperature (20 °C).

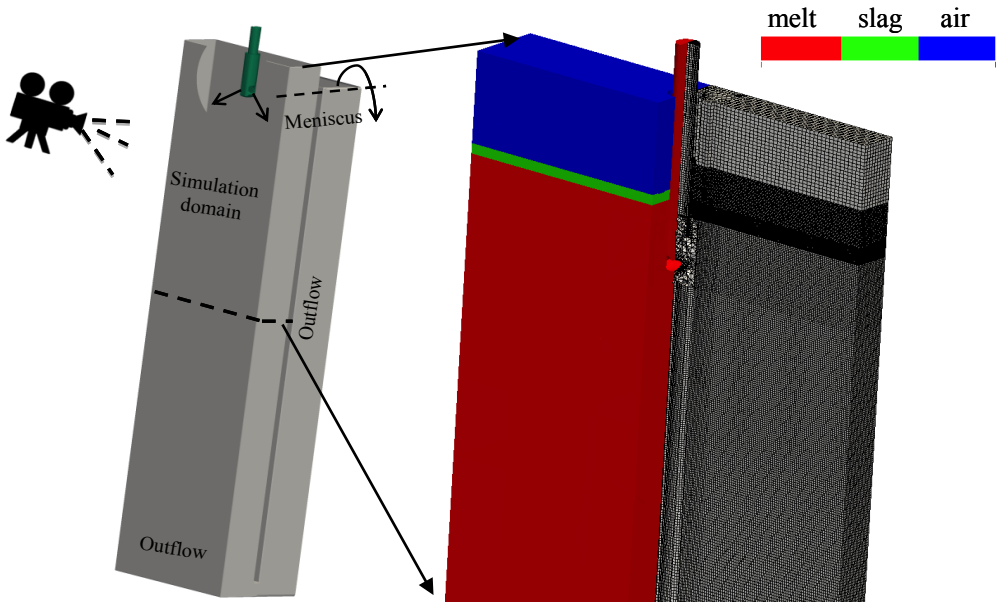

a) b) c)

Fig. 2. Experimental/simulation setup: (a) mold with SEN and outflow system in the water modeling experiment; (b) initial phase distribution in the simulation; (c) details of the numerical mesh.

In this paper only results from the water modeling system are described in detail. Different casting speeds were tested, ranging from minimal when the liquid slag/melt interface was almost undisturbed up to the maximum casting speed when intensive slag entrapment was observed. Only the results with the maximum casting speed are analyzed in the following sections.

Table 1. Material properties and throughput in the CC process and water modeling experiment

Parameter	Steel	Slag	Water	Oil	Air
Molecular viscosity, μ (kg/m·s)	$5.6 \cdot 10^{-3}$	-	$1.0 \cdot 10^{-3}$	0.53	$1.82 \cdot 10^{-5}$
Density, ρ (kg/m^3)	7000	2700	1000	921	1.205
Kinematic viscosity, $\eta = \mu/\rho$ (m^2/s)	$8.0 \cdot 10^{-7}$	-	$1.0 \cdot 10^{-6}$	$5.8 \cdot 10^{-4}$	$1.51 \cdot 10^{-5}$
Casting speed (m/min)	1.5		4.5		
Throughput (m^3/h)	28.1		9.4		

The mold/SEN system design is schematically represented in Fig. 2(a). It included a vertical model of a conventional CC mold that was connected at the bottom to an outflow system, which was opened and thereby naturally maintained the meniscus level. The SEN was mounted in the top of the mold and provided the desired water throughput.

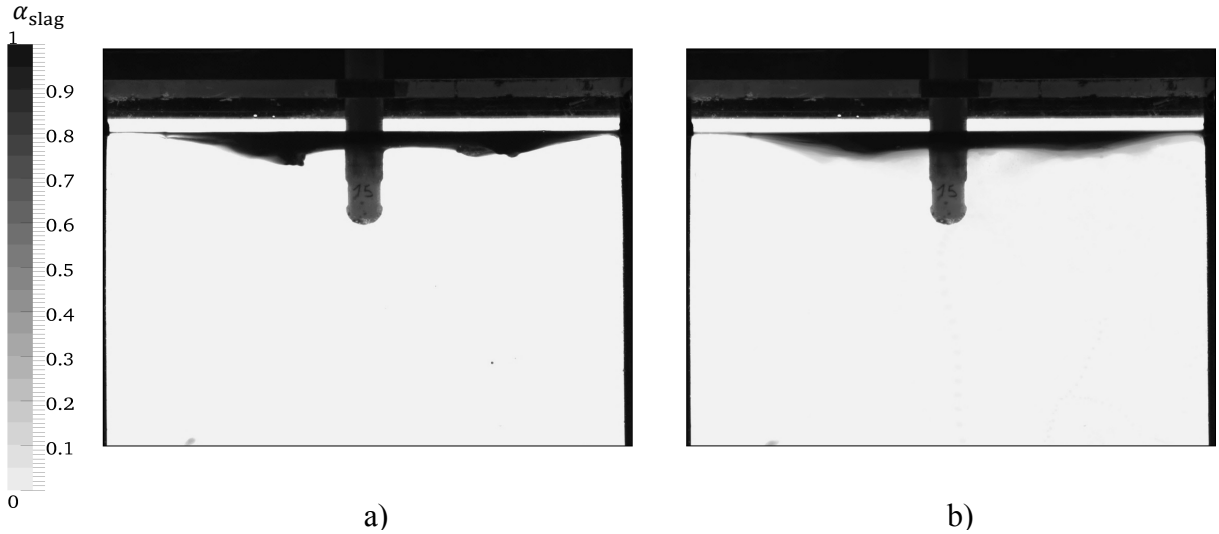

Fig. 3. Experimentally measured oil phase distribution: (a) an instantaneous snapshot and (b) a time-averaged image.

A special SEN design was used in the current study that provides very stable flowing jets coming out of the SEN ports.

The experimental procedure was performed in the following manner:

1. Mineral oil was poured on top of the still water and allowed to float up to form a uniform layer approx. 10 mm thick.
2. Water flow through the SEN was started and adjusted until the volumetric throughput reached steady state.
3. An experimental run was performed using a digital camera to record the oil layer position, possible entrapment of oil droplets and swirl formation near the SEN.

The sequence of images acquired during experiments was recorded, and an example of the snapshot of the oil phase distribution is shown in Fig. 3(a). Additionally, post-processing of the images was performed to obtain a time-averaged oil phase distribution, as shown in Fig. 3(b).

4. Simulation results

The simulation domain was limited to 2 m in the upper mold region (Fig. 2(b)) to avoid huge computational expense on very large grids.

The results of the simulation are displayed in Fig. 4, namely the instantaneous slag position in black with the velocity vector field representing the flow directions, the magnitude of the mixture velocity in the center plane and the streamlines, showing the flow complexity inside the simulation domain, and oscillations of the slag layer.

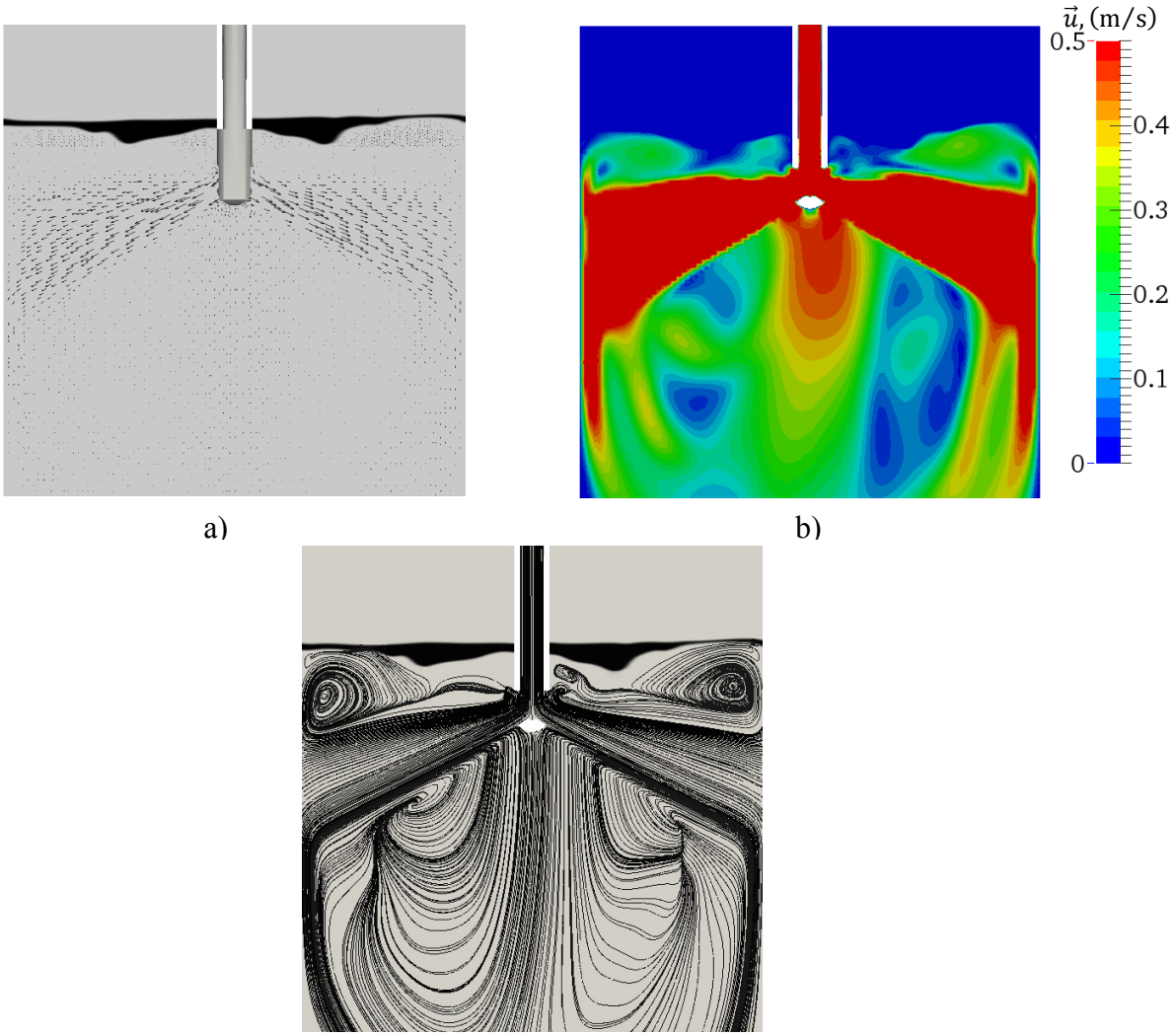

Fig. 4. Oil layer distribution and velocity field (a), velocity magnitude distribution (b) and the flow streamlines (c) in the center plane.

One issue should be highlighted: due to the low air viscosity and intensive momentum transfer from the water and slag layer to the air phase, the air velocity was over-predicted. This high air velocity did not influence the calculation of the slag and water regions significantly, but a high Courant number appeared in the air region that slowed down the calculation. The solution to this issue was quite simple: the momentum conservation equation was reduced in the air by limiting it to the diffusion mechanism by multiplying the convective term on the left-hand side of the equation (6) by $(1 - \alpha_{\text{air}})$ as follows:

$$\frac{\partial \rho \vec{u}}{\partial t} + (1 - \alpha_{\text{air}})\, \nabla \cdot (\rho \vec{u} \otimes \vec{u}) = -\nabla p + \nabla \cdot (2\mu_{\text{eff}} \mathbf{D}) + \rho \vec{g} + \vec{S}_{\text{surf}} \quad (17)$$

Consequently the velocities and turbulence level in the air region were reduced, as evident in Fig. 5. The turbulence kinetic energy field is shown for the middle plane based on the results obtained with the standard (Fig. 5(a)) and improved (Fig.5(b)) models.

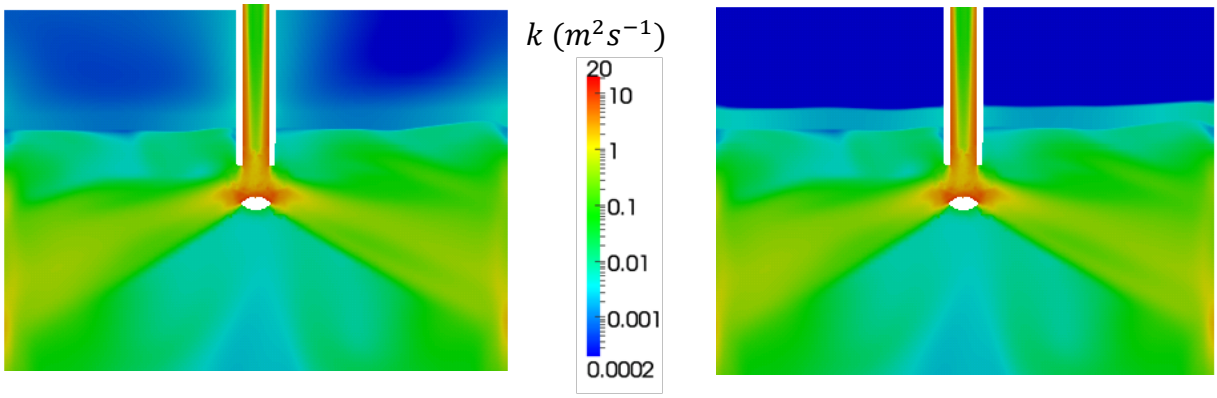

a) b)

Fig. 5. Dumping the turbulence in the air region: (a) standard model and (b) the convective term modified in the air region.

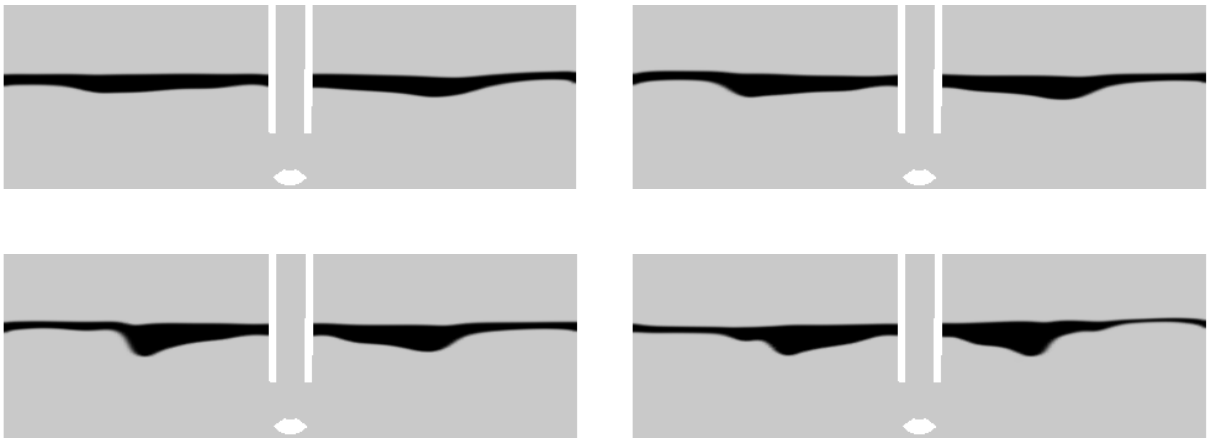

Fig. 6. Evolution of the slag position at different time points according to the numerical simulation.

The dynamics of the simulated slag layer distribution are shown in Fig. 6, visualizing how the interface was deformed by the flow: starting from a completely flat interface it was gradually deformed by the upper rolls of the melt flow (Fig. 4(c)).

5. Discussion

After the numerical model was established and the multiphase solver was developed and tuned, verification of the VOF modeling was performed.

In the first stage a time-averaged gray-scaled image was obtained (Fig. 3(b)). Using the open-source graphic tool all the experimental images in the series were blended using the uniform weighting factor. Applying additional threshold filters to the time-averaged image, a boundary of the most stable region was determined. It is marked as a red line in Fig. 7 and

compared with the time-averaged slag distribution from the water modeling in Fig. 7(a) and with the time-averaged slag distribution from the numerical simulation in Fig. 7(b).

It is evident that even if the SEN design provides a very stable flow, the slag interface is highly distorted due to the high sub-meniscus velocities. As mentioned previously, an extreme case of maximum casting speed was examined.

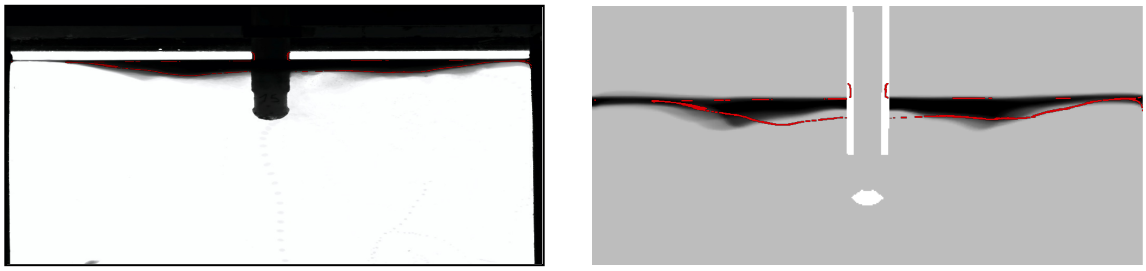

a) b)

Fig. 7. Comparison of the time-averaged slag distribution from the water modeling experiment (a) with results from the numerical simulation (b). The time-averaged interface position from the water modeling, after applying additional threshold filters, is marked as a red line on the numerical simulation.

The numerical simulation setup was verified regarding the importance of the following VOF model parameters:

- surface tension between phases;
- contact angles at the walls.

It was found that the contact angle doesn't play an important role when critical casting speeds are dealt with and the dominant flow is highly convective. Therefore some default values can be used. In a 3-phase water/oil/air system the most important parameter is the surface tension between the water and oil. The aim of the studies was to find an appropriate value for the surface tension.

It was observed that the surface tension for the interface between air and other phases did not have such a dramatic influence on the simulation results, hence the standard value of 0.07 N/m for the air/water and air/oil interface was used. The interface free energy σ was varied for the water/oil phase pair in the range from 0.02–0.5 N/m, as reported in literature [14]. It was observed that for the lowest value, the slag layer was washed away immediately by the flow due to its low resistance to the shear forces. On the other hand, for the highest values of σ (around 0.5 N/m) the surface tension was too strong, dragging the slag and causing it to gather together and form a ring around the SEN at the end of the simulation leaving the entire meniscus open to the air.

The optimal value was found to be around 0.07 N/m and the time averaged results gave quite good qualitative agreement with the experimental data (see Fig. 7(b)). A better match with the experimental results could be achieved using an additional mesh refinement strategy and by obtaining the flow pattern from the water model using tracers, dye injection etc.

6. Summary

A numerical approach (VOF model, OpenFOAM® open-source CFD package) was used to model the 3-phase liquid steel/slag/air system during continuous casting. The water modeling experiment was performed to verify the computational method. A time-averaged oil-water interface position was obtained from the water modeling and compared with the numerical results. The surface tension (interface free energy) was varied in the simulation to match the experimental oil distribution profiles, because values for the water-oil interface free

energy reported in literature are scattered (~ 0.02–0.5 N/m). A quite good qualitative agreement was achieved with a water-oil interface free energy of 0.07 N/m. However, reliability of this interface free energy and contact angle at some triple points, as well as sensitivity of the final modeling result to these parameters need to be further verified.

In future work additional experiments should be performed to obtain the 3D flow pattern. The actual water-oil interface profile is a complex 3D feature, but the images obtained using the digital camera only provide 2D information. Some important information in the third dimension concerning the turbulent flow and its interaction with the oil is missing with the current approach.

From the modeling perspective, local mesh adaptation (refinement) should be performed to examine the slag (droplets) entrainment since the convective schemes became too diffuse on the coarse (for the droplets size) mesh. An alternative approach based on an initial fine grid is not acceptable due to the extremely high computational costs.

Acknowledgment

The financial support provided by RHI AG, the Austrian Federal Ministry of Economy, Family and Youth and the National Foundation for Research, Technology and Development in the framework of Christian-Doppler Laboratory "Advanced Process Simulation of Solidification and Melting" is gratefully acknowledged.

References

[1] M. Cross, K. Pericleous, T.N. Croft et al., Computational modeling of mold filling and free-surface flows in shape casting: an overview of the challenges involved, Metall. & Materials Trans. B, 37B (2006), pp. 879–885

[2] OpenFOAM® V2.1.1 Documentation http://www.openfoam.org/archive/2.1.1/docs/

[3] H. Rusche, Computational fluid dynamics of dispersed two-phase flows at high phase fractions, Ph.D. Thesis, Imperial College of Science, Technology and Medicine, 2002

[4] C. W. Hirt, B. D. Nichols, Volume of fluid (VOF) method for the dynamics of free boundaries, J. Comp. Phys., 39 (1981), pp. 201–225

[5] S. Osher, J. A. Sethian, Fronts propagating with curvature-dependent speed: algorithms based on Hamilton–Jacobi formulations, J. Comp. Phys., 79 (1988), pp. 12–49

[6] D. Jacquim, Calculation of two-phase Navier-Stokes flows using phase-field modeling, J. Comp. Physics, 155 (1999), pp. 96–127

[7] J. U. Brackbill, D. B. Kothe, C. Zemach, A continuum method for modelling surface tension, J. Comp. Physics, 100 (1992), pp. 335–354

[8] V. R. Gopala, B. G. M. van Wachem, Volume of fluid methods for immiscible-fluid and free-surface flows, Chem. Eng. J., 141 (2008), pp. 204–221

[9] J. C. G. Verschaeve, High order interface reconstruction for the volume of fluid method, Computers & Fluids, 46 (2011), pp. 486–492

[10] M. Sussman, K.M. Smith, M.Y. Hussaini, M. Ohta, R. Zhi-Wei, A sharp interface method for incompressible two-phase flows, J. Comp. Physics, 221 (2007), pp. 469–505

[11] J. Klostermann, K. Schaake, R. Schwarze, Numerical simulation of a single rising bubble by VOF with surface compression, Int. J. Numer. Meth. Fluids, 71 (2013), pp. 469–505

[12] O. Ubbink, Numerical prediction of two fluid systems with sharp interfaces, Ph.D. Thesis, Imperial College of Science, Technology and Medicine, 1997

[13] O. Ubbink, R.I. Issa, A method for capturing sharp fluid interfaces on arbitrary meshes, J. Comp. Physics, 153 (1999), pp. 26–50

[14] John A. Dean, N. A. Lange, Handbook of chemistry, McGraw-Hill (1999), p. 1424